Diese Arbeit wurde vorgelegt am
Lehr- und Forschungsgebiet: Kontinuierliche Optimierung (IGPM)

Regelung der Temperatur in Rohrnetzwerken Solarthermischer Kraftwerke

Control of the Temperature in a Network of Tubes of Solar Thermal Power Plants

Bachelorarbeit
Computational Engineering Science

August 2018

Vorgelegt von Presented by	Matthias Cherek Lemierser Straße 4 52074 Aachen Matrikelnummer: 320746 matthias.cherek@rwth-aachen.de
Erstprüfer First examiner	Prof. Dr. rer. nat. Michael Herty Lehr- und Forschungsgebiet: Kontinuierliche Optimierung (IGPM) RWTH Aachen University
Externer Betreuer External supervisor	Dr. rer. nat. Pascal Richter Steinbuch Centre for Computing Karlsruhe Institute of Technology

Eigenständigkeitserklärung

Hiermit versichere ich, dass ich diese Bachelorarbeit selbständig verfasst und keine anderen als die angegebenen Quellen und Hilfsmittel benutzt habe. Die Stellen meiner Arbeit, die dem Wortlaut oder dem Sinn nach anderen Werken entnommen sind, habe ich in jedem Fall unter Angabe der Quelle als Entlehnung kenntlich gemacht. Dasselbe gilt sinngemäß für Tabellen und Abbildungen. Diese Arbeit hat in dieser oder einer ähnlichen Form noch nicht im Rahmen einer anderen Prüfung vorgelegen.

Aachen, im August 2018

Matthias Cherek

Contents

List of Figures

List of Tables

1 Introduction

The need for electrical energy grows steadily with the technological progress and especially, with third world countries catching up to a higher standard [1]. Climate change is also a big and growing challenge to the energy sector. This puts a lot of pressure on the development of regenerative energy sources. These sources not only have to produce enough energy but must also be profitable. In this sense it is very important to maximize the efficiency of power plants producing green energy. There are many types of those power plants. Concentrating solar thermal power plants are a promising way of regenerative energy production and they are being build more and more often in the last ten years [2].
This thesis will deal with solar thermal power plants with parabolic trough technology. They produce steam and generate energy through a turbine just like classical power plants. The steam is generated by a heat exchanger with a heat transfer fluid (HTF). This fluid is heated in long absorber tubes. Along these tubes collectors concentrate sun beams onto them (see Figure 1), so the fluid is heated up significantly.
These plants consist of a large number of collector rows. The task of improving these plants is to maximize the mass flow of heated fluid that enters the heat exchanger. The more fluid with its temperature close to the maximum enters the heat exchanger, the more steam can be generated. Additionally, the HTF must never exceed the desired temperature. If the temperature gets too high the HTF will irreversibly chemically decompose. Modern control schemes regulate the flow of fluid through the network of tubes with the pump and defocus mirrors from the collector field if the HTF becomes too hot. In this thesis a way of improving the temperature control of solar thermal power plants is introduced. In detail the volume flow through each absorber tube will be controlled using the built-in valves at the inflow section. The goal is to reduce the defocus time of the mirrors. The concept of solar thermal power plants with collector rows can be seen in Figure 2. The simulation in this thesis will only consist of the left part labeled as parabolic trough collector.

In the following section a brief overview over the current technology will be provided. In Section 3 the optical model, representative of the energy input from the sun, along with the geometrical parameters of the plant will be presented. Section 4 deals with the thermodynamic model, describing the processes of the HTF in the tubes and in Section 5 the network model, which provides coupling conditions for the behavior of the HTF in the junctions where the tubes are connected, will be discussed. Two different ways of controlling the temperature in a network of tubes will be shown in Section 6 and Section 7, the mirror control, which represents the state-of-the-art control, and the valve control. The mirror control consists of a static proportional-integral-differential (PID) controller for the pump and a system to defocus mirrors from the collector field. The valve control uses the same PID controller but changes the volumetric flow through the pipes utilizing the valves. In Section 8 three different test cases are presented and their results evaluated.

Figure 1: A collector row of a solar thermal power plant. The mirrors concentrate the sun beams onto the tube in which the HTF (thermal oil/molten salt) is heated.

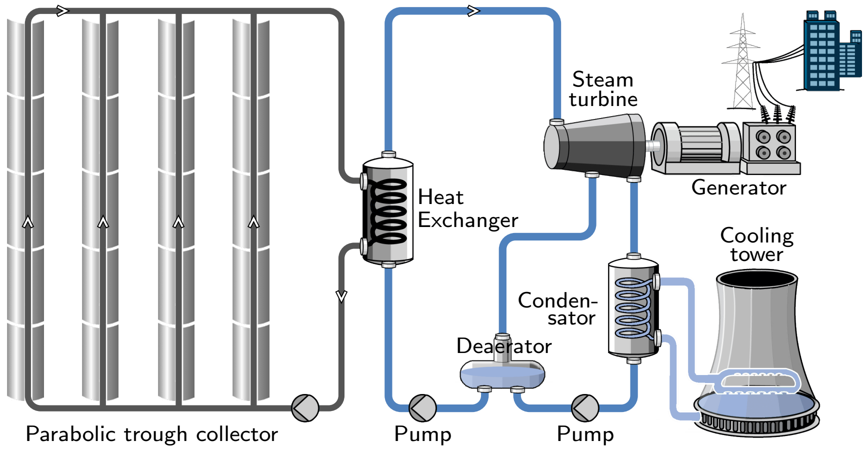

Figure 2: Conceptual drawing of a solar thermal parabolic trough power plant. The HTF is heated in the parabolic trough collector field. With this energy steam is generated in the heat exchanger which then powers a steam turbine. The water is cooled down and condensed before entering the heat exchanger again. The HTF enters the parabolic trough collector field again after heating the water.

2 State of the art

There has already been a lot of research on the topic of controlling the temperature in solar thermal power plants [3]. The focus of this research lies on the control schemes for the pump. There are many different approaches to advanced control mechanism. Adaptive control tries to modify the behavior of the controller if the process dynamics change. If the controller variables can be calculated directly from the process variables these controllers are called gain-scheduling controllers. Time delay compensation schemes focus on the effect of dead-times in a process which appear in many industrial applications [4] that include mass and or energy-transport. If discrepancies between the model and the reality should be considered a robust control strategy is a possible choice. It consists of a feedback system between the plant and the controller. There are many more schemes like predictive control, fuzzy logic control, control with neural networks and monitoring and hierarchical control. Most of these schemes focus on controlling the temperature in a single pipe by changing the volumetric flow of the pump as in [5]. This is due to the fact that these schemes are easily expandable to more tubes since they defocus mirrors if the fluid in a tube becomes too hot. As a result, the current technology used in controlling solar thermal trough plants is mainly used to avoid variations in the temperature. This increases the efficiency of the plant because the desired temperature T_{out} in the tubes is reached more reliably. If this was not the case the plant would have to be run in a setting that assures the desired temperature is never exceeded by keeping the fluid colder than it has to be to anticipate variations. Another way of increasing the efficiency of the plant would be to minimize the time and number of defocused mirrors and thus increasing the energy input from the sun. This is the approach this thesis takes.

3 Optical model

The energy input in the system of tubes of a solar thermal power plant comes from the sun. To be able to simulate the whole system we need to model it to observe the behavior of the system and the controller.

3.1 Solar irradiation from the sun on the collector field

The direct normal solar irradiation I is the intensity of the sun in Watt per square meter. It varies over the course of a day and usually reaches its maximum around noon [3]. That means that I is time dependent. The solar irradiation can also change over space. If clouds overshadow parts of the plant the intensity changes only there,

$$I = I(x,t)\,. \tag{1}$$

The control schemes that are developed in this thesis are static. That means the time dependency is not of interest for the final results,

$$I = I(x)\,. \tag{2}$$

The solar irradiation will be modeled for each tube independently and spatially discretized. This allows the simulation of partially overshadowed absorber tubes.

3.2 Parameters for the mirrors in the collector field

Additionally to the solar irradiation itself there are other variables in the optical model. The efficiency of the mirrors η_{col} will be modeled as a global factor,

$$\eta_{\text{col}} \in [0,1]\,. \tag{3}$$

The aperture of the mirror G is the width of the collector visible in Figure 1 in meter. In order to be able to defocus mirrors from the collector field another variable has to be introduced. The defocus factor ϕ states if a mirror in the collector field is defocused or not. For that it must be spatially discretized for each tube individually. For a defocused mirror it takes the value zero and for a focused one the value one. For the header tubes in the network it takes the value zero for the whole tube,

$$\phi(x) = 1 \vee \phi(x) = 0\,. \tag{4}$$

3.3 Geometrical parameters for the collector field

The geometry of the plant is very important in modeling the collector field because it influences the behavior of the HTF and the energy input significantly.
A solar thermal parabolic trough power plant consists of N collector rows or absorber tubes and two header tubes. The HTF enters through the pump into the inflow header-tube and is distributed into the absorber tubes. After being heated up the HTF enters

the outflow header-tube which transports it into the heat exchanger. The length of the absorber tubes ℓ_a is determined by the length and number of mirrors per collector row,

$$\ell_\mathrm{a} = \ell_\mathrm{mirror} \cdot N_\mathrm{mirror} \,. \tag{5}$$

The length of the header tubes ℓ_h is determined by the number of absorber tubes N and the distance between each absorber tube ℓ_d,

$$\ell_\mathrm{h} = N \cdot \ell_\mathrm{d} \,. \tag{6}$$

The cross sectional area of the header tube A_h and the absorber tube A_a must also be specified. From these the inner diameter of the absorber and header tubes D_a and D_h can be calculated,

$$D_\mathrm{a} = \sqrt{\frac{A_\mathrm{a}}{\pi}} \cdot 2 \,, \tag{7}$$

$$D_\mathrm{h} = \sqrt{\frac{A_\mathrm{h}}{\pi}} \cdot 2 \,. \tag{8}$$

Altogether for the optical and geometrical model the parameters listed in Table 1 need to be specified.

Parameter	**Description**	**Unit**
$I(x)$	Direct solar irradiation	$\mathrm{W\,m^{-2}}$
η_col	Global efficiency factor	-
G	Aperture of the mirrors	m
$\phi(x)$	Defocus factor	-
N	Number of collector rows	-
N_mirror	Number of mirrors per collector row	-
ℓ_a	Length of the collector rows	m
ℓ_mirror	Length of the mirrors	m
ℓ_h	Length of the header tubes	m
ℓ_d	Distance between the absorber tubes	m
A_h	Cross sectional area of the header tubes	$\mathrm{m^2}$
A_a	Cross sectional area of the absorber tubes	$\mathrm{m^2}$
D_h	Inner diameter of the header tubes	m
D_a	Inner diameter of the absorber tubes	m

Table 1: All parameters that must be specified for the optical and geometrical model of the solar thermal parabolic trough power plant.

4 Thermodynamic model

The behavior of the HTF in the tubes is dominated by the thermodynamic processes. In this section a model for the HTF is derived. Additionally, a finite volume method for solving the derived equation is presented.

4.1 Equations

The flow of a fluid can be described by the conservation laws for mass, momentum and energy. Using the conservation laws in [6] the flow of a fluid in a tube was derived. In [3] a model for the energy input from the sun is given. The flow is modeled as one-dimensional because the diameter of typical absorber tubes is five magnitudes smaller than their length, so we assume that the changes in the y- and z-direction are negligible. Combining these equations yields the following system of equations,

$$\rho_t + (\rho u)_x = 0 \,, \tag{9}$$

$$(\rho u)_t + (\rho u^2 + p)_x = -\frac{\xi}{D}\frac{\rho u|u|}{2} + \frac{4}{3}(\mu u_x)_x \,, \tag{10}$$

$$E_t + (u(E+p))_x = \frac{\omega}{D}\frac{\rho u^2|u|}{2} + \frac{4}{3}(\mu u u_x)_x + (kT_x)_x + \frac{4}{D}H^{\mathrm{t}}(T_{\mathrm{m}} - T) \,, \tag{11}$$

$$\rho_{\mathrm{m}} c_{\mathrm{m}} A (T_{\mathrm{m}})_t = \eta_{\mathrm{col}} G I(x)\phi(x) - P_{\mathrm{rc}} - D\pi H^{\mathrm{t}}(T_{\mathrm{m}} - T) \,. \tag{12}$$

Here ρ is the density of the fluid, u the velocity of the fluid, p the pressure of the fluid, ω the surface roughness of the tube, μ the dynamic viscosity of the fluid, E the total energy of the fluid, k the thermal conductivity of the fluid, T the temperature of the fluid, H^{t} the convective heat transfer coefficient, T_{m} the temperature of the tube wall, ρ_{m} the density of the tube wall, c_{m} the specific heat capacity of the tube wall and P_{rc} the convective thermal losses.
Equations (9), (10) and (11) describe the conservation laws of mass, momentum and energy and (12) the temperature of the wall of the tubes. In equation (10) three different forces were included, pressure forces, friction forces with the tube and inner friction forces. In equation (11) the effects of pressure forces, dissipation, inner heat transfer and temperature exchange with the tube were modeled. Equation (12) includes the solar irradiation, heat losses and temperature exchange with the fluid.

The convective heat transfer coefficient H^{t} can be expressed as [3]

$$H^{\mathrm{t}} = H_{\mathrm{v}} \left(u \tfrac{D^2}{4} \pi \right)^{0.8} \tag{13}$$

with

$$H_{\mathrm{v}} = 2.17 \cdot 10^6 - 5.01 \cdot 10^4 T + 4.53 \cdot 10^2 T^2 - 1.64 T^3 + 2.1 \cdot 10^{-3} T^4 \,. \tag{14}$$

Since it is our goal to observe and control the temperature of the fluid, we rewrite equation (11) so that it models the temperature instead of the total energy of the system. To do that we look at the definition of the total energy E

$$E = \rho \left(c_{\mathrm{v}} T + \tfrac{u^2}{2} + gH \right) \tag{15}$$

with the specific heat capacity of the HTF c_{v} the gravitational acceleration of the earth g and the height H. We can neglect the gravitational energy gH because the plant is nearly horizontal. By inserting equation (15) in (11) we obtain

$$\left(\rho \left(c_{\mathrm{v}} T + \frac{u^2}{2} \right) \right)_t + \left(u \left(\rho \left(c_{\mathrm{v}} T + \frac{u^2}{2} \right) + p \right) \right)_x = \frac{\omega}{D} \frac{\rho u^2 |u|}{2} + \frac{4}{3} (\mu u u_x)_x + (k T_x)_x + \frac{4}{D} H^{\mathrm{t}} (T_{\mathrm{m}} - T). \tag{16}$$

4.2 Closure equations for the thermodynamic model

To specify which fluid is used we have to choose equations of state for the thermodynamic model. In this thesis we will use molten salt [7] and Therminol VP1 [8]. We have to provide equations for the density ρ, the dynamic viscosity μ, the thermal conductivity k, the specific heat capacity c_v and the temperature T.

4.2.1 Molten Salt

The equations for molten salt are given in [7] as polynomials of the temperature,

$$\rho(T) = 2293.6 - 0.7497 T\,, \tag{17}$$

$$\mu(T) = 0.4737 - 2.297 \cdot 10^{-3} T + 3.731 \cdot 10^{-6} T^2 - 2.019 \cdot 10^{-9} T^3\,, \tag{18}$$

$$k(T) = 0.6966 - 4.6055 \cdot 10^{-4} T\,, \tag{19}$$

$$c_v(T) = 5806 - 10.833 T + 7.2413 \cdot 10^{-3} T^2\,. \tag{20}$$

By inverting the equation for the density we obtain an expression for the temperature dependent on the density,

$$T(\rho) = 3059.357 - 1.3339 \rho\,. \tag{21}$$

4.2.2 Therminol VP1

The equations for Therminol VP1 are given in [8] as polynomials of the temperature,

$$\rho(T) = -\,0.90797\,(T - 273.15) + 0.00078116\,(T - 273.15)^2$$

$$- 2.367 \cdot 10^{-6} \, (T - 273.15)^3 + 1083.25 \,, \tag{22}$$

$$\mu(T) = \exp\left(\frac{544.149}{(T - 273.15) + 114.43} - 2.59578 \right) \cdot 10^{-6} \, \rho \,, \tag{23}$$

$$\begin{aligned} k(T) = & - 8.19477 \cdot 10^{-5} \, (T - 273.15) - 1.92257 \cdot 10^{-7} \, (T - 273.15)^2 \\ & + 2.5034 \cdot 10^{-11} \, (T - 273.15)^3 - 7.2974 \cdot 10^{-15} \, (T - 273.15)^4 \\ & + 0.137743 \,, \end{aligned} \tag{24}$$

$$\begin{aligned} c_v(T) = & (0.002414 \, (T - 273.15) + 5.9591 \cdot 10^{-6} \, (T - 273.15)^2 \\ & - 2.9879 \cdot 10^{-8} \, (T - 273.15)^3 \\ & + 4.4172 \cdot 10^{-11} \, (T - 273.15)^4 + 1.498) \cdot 10^3 \,. \end{aligned} \tag{25}$$

Since the density $\rho(T)$ is a non linear equation we can not simply invert it to observe an equation for the temperature. To solve this problem we will calculate the solution with an iterative Newtons method,

$$T_{n+1} = T_n - \frac{\rho(T_n) - \rho}{\rho'(T_n)} \,. \tag{26}$$

4.3 Scale analysis

The results of the simulation depend on their dimensions. To examine the different influences of each part of the equations on the results we derive a scaled version of the partial differential equation system (9), (10), (**??**). This was already done in [6] with a different set of reference parameters. We use the set of reference parameters with index r shown in Table 2 and Table 3. The scaled version of (9), (10), (**??**) with the magnitude of each factor is shown below,

$$\rho_t + (\rho u)_x = 0 \,, \tag{27}$$

$$(\rho u)_t + \left(\rho u^2 + \overbrace{\frac{p_\mathrm{r}}{\rho_\mathrm{r} u_\mathrm{r}^2}}^{\text{salt: } 10^3 \text{ oil: } 10^3} p \right)_x = - \overbrace{\frac{\omega}{D_\mathrm{a}} \ell_\mathrm{a}}^{\text{salt: } 10^2 \text{ oil: } 10^2} \frac{\rho u |u|}{2} + \frac{4}{3} \overbrace{\frac{\mu_\mathrm{r}}{\rho_\mathrm{r} \ell_\mathrm{a} u_\mathrm{r}}}^{\text{salt: } 10^{-9} \text{ oil: } 10^{-10}} (\mu u_x)_x \,, \tag{28}$$

$$\left(\rho \left(T + \overbrace{\frac{u_\mathrm{r}^2}{T_\mathrm{r} c_\mathrm{v}}}^{\text{salt: } 10^{-7} \text{ oil: } 10^{-6}} \frac{u^2}{2} \right) \right)_t + \left(u\rho \left(T + \overbrace{\frac{u_\mathrm{r}^2}{T_\mathrm{r} c_\mathrm{v}}}^{\text{salt: } 10^{-7} \text{ oil: } 10^{-6}} \frac{u^2}{2} \right) + \overbrace{\frac{p_\mathrm{r}}{\rho_\mathrm{r} T_\mathrm{r} c_\mathrm{v}}}^{\text{salt: } 10^{-4} \text{ oil: } 10^{-2}} p u \right)_x$$

$$= \overbrace{\frac{\omega}{D_\mathrm{a}} \frac{u_\mathrm{r}^2 \ell_\mathrm{a}}{c_\mathrm{v} T_\mathrm{r}}}^{\text{salt: } 10^{-4} \text{ oil: } 10^{-4}} \frac{\rho u^2 |u|}{2} + \overbrace{\frac{\mu_\mathrm{r} u_\mathrm{r}}{\rho_\mathrm{r} \ell_\mathrm{a} c_\mathrm{v} T_\mathrm{r}}}^{\text{salt: } 10^{-15} \text{ oil: } 10^{-15}} \frac{4}{3} (\rho \mu u_x u)_x + \overbrace{\frac{k_\mathrm{r}}{\rho_\mathrm{r} c_\mathrm{v} u_\mathrm{r} \ell_\mathrm{a}}}^{\text{salt: } 10^{-10} \text{ oil: } 10^{-11}} (k T_x)_x$$

$$- \overbrace{\frac{4H_{\mathrm{r}}^{\mathrm{t}}T_{\mathrm{m,r}}}{D_{\mathrm{a}}\rho_{\mathrm{r}}c_{\mathrm{v}}T_{\mathrm{r}}}}^{\text{salt: }10^1\text{ oil: }10^1} H^{\mathrm{t}}T_{\mathrm{m}} + \overbrace{\frac{4H_{\mathrm{r}}^{\mathrm{t}}}{D_{\mathrm{a}}\rho_{\mathrm{r}}c_{\mathrm{v}}}}^{\text{salt: }10^1\text{ oil: }10^1} H^{\mathrm{t}}T\,. \tag{29}$$

Quantity		**Value**
Length of the absorber tube	ℓ_{a}	1000 m
Inner diameter of the absorber tube	D_{a}	0,070 m
Inner diameter of the header tube	D_{h}	0,1 m
Surface roughness	ω	0,024 mm

Table 2: Reference parameters for the network of tubes. These parameters do not depend on the HTF.

Quantity		**Molten salt**	**Thermal oil**	**Unit**
Temperature	T_{r}	[523.2, 710]	[353.2, 673.2]	K
Pressure	p_{r}	[1, 10]	[70, 100]	bar
Velocity	u_{r}	[0.68, 0.74]	[1.28, 1.87]	$\mathrm{m\,s^{-1}}$
Temperature of the wall	$T_{\mathrm{m,r}}$	[523.2, 710]	[353.2, 673.2]	K
Heat transfer coefficient	$H_{\mathrm{r}}^{\mathrm{t}}$	[2023400, 200450]	[1299100, 193490]	$\mathrm{W\,m^{-2}\,K^{-1}}$
Density	ρ_{r}	[1901.4, 1761.3]	[1014.4, 693.6]	$\mathrm{kg\,m^{-3}}$
Dynamic viscosity	μ_{r}	[0.0041, 0.0010]	[0.0012, 0.00015]	$\mathrm{kg\,m^{-1}\,s^{-1}}$
Specific heat	c_{v}	[2120.6, 1764.9]	[1715.8, 2635.6]	$\mathrm{m^2\,s^{-2}\,K^{-1}}$
Thermal conductivity	k_{r}	[0.4557, 0.3696]	[0.1300, 0.0756]	$\mathrm{W\,m^{-1}\,K^{-1}}$

Table 3: Reference parameters for the HTF. The parameters are given for molten salt and thermal oil in a range that is typical for the use in solar thermal power plants.

If we compare the magnitude of the scale factors we can see that some parts have a very small impact on the results and can be neglected. In (28) the last factor is far smaller than the rest. In (29) all factors with a magnitude of 10^{-6} or smaller are neglected. When we eliminate these terms we obtain the following system of equations,

$$\rho_t + (\rho u)_x = 0\,, \tag{30}$$

$$(\rho u)_t + \left(\rho u^2 + \frac{p_{\mathrm{r}}}{\rho_{\mathrm{r}}u_{\mathrm{r}}^2}p\right)_x = -\frac{\omega}{D_{\mathrm{a}}}\ell_{\mathrm{a}}\frac{\rho u|u|}{2}\,, \tag{31}$$

$$(\rho T)_t + \left(u\rho T + \frac{p_{\mathrm{r}}}{\rho_{\mathrm{r}}T_{\mathrm{r}}c_{\mathrm{v}}}pu\right)_x = \frac{\xi}{D_{\mathrm{a}}}\frac{u_{\mathrm{r}}^2\ell_{\mathrm{a}}}{c_{\mathrm{v}}T_{\mathrm{r}}}\frac{\rho u^2|u|}{2} - \frac{4H_{\mathrm{r}}^{\mathrm{t}}T_{\mathrm{m,r}}}{D_{\mathrm{a}}\rho_{\mathrm{r}}c_{\mathrm{v}}T_{\mathrm{r}}}H^{\mathrm{t}}T_{\mathrm{m}} + \frac{4H_{\mathrm{r}}^{\mathrm{t}}}{D_{\mathrm{a}}\rho_{\mathrm{r}}c_{\mathrm{v}}}H^{\mathrm{t}}T\,. \tag{32}$$

4.4 Simplified model

Equations (30),(31) and (32) are still a system of three partial differential equations (PDEs). To reduce complexity and computation time we would like to reduce the system to a single PDE. Such an equation is described in [3]. We can derive this model from our system if an incompressible flow with negligible axial conduction is assumed. Additionally the equations for mass and momentum can be neglected. The behavior of the HTF in the pipe is dominated by the energy input from the sun and thus the energy is the leading parameter in the system. This step includes eliminating the pressure from the model so that there is no pressure model needed to solve the equation. The obtained equations are

$$\rho c_{\mathrm{v}} T_t + \rho c_{\mathrm{v}} u T_x = \frac{4}{D} H^{\mathrm{t}} (T_{\mathrm{m}} - T) \,, \tag{33}$$

$$\rho_{\mathrm{m}} c_{\mathrm{m}} A (T_{\mathrm{m}})_t = \eta_{\mathrm{col}} G I(x) \phi(x) - P_{\mathrm{rc}} - D \pi H^{\mathrm{t}} (T_{\mathrm{m}} - T) \,. \tag{34}$$

In [9] this model was implemented and the results were compared to real data. The comparison showed that the differences were negligible small. Neglecting heat losses and diffusion [9] the energy balance can be further simplified,

$$P_{\mathrm{rc}} = 0, \; (T_{\mathrm{m}})_t = 0 \,. \tag{35}$$

The finally obtained model,

$$T_t + u T_x = \frac{\eta_{\mathrm{col}} G}{\rho c_{\mathrm{v}} A} I(x) \phi(x) \,, \tag{36}$$

is also used by many authors [5, 10, 11]. To be able to consider thermodynamic losses we introduce a thermodynamic efficiency factor η_{therm},

$$\eta_{\mathrm{therm}} \in [0, 1] \,. \tag{37}$$

It is included in the source term of equation (36),

$$T_t + u T_x = \frac{\eta_{\mathrm{col}} \eta_{\mathrm{therm}} G}{\rho c_{\mathrm{v}} A} I(x) \phi(x) \,. \tag{38}$$

4.5 Solver

In order to simulate the solar thermal power plant we have to solve equation (38). We will do that numerically with a finite volume method.
By analyzing equation (38) it can be seen, that the information is only transported in positive x-direction since the velocity u is strictly positive. In this case an upwind scheme is a good choice. The method we use for solving the homogeneous part of equation (38) is the following

$$T_i^{n+1,-} = T_i^n - \Delta t \, (u \, T_x^-) \,, \tag{39}$$

with the indices i for the cell and n for the current time step. Δt is the time step size. T_x^- is defined as

$$T_x^- = \frac{T_i^n - T_{i-1}^n}{\Delta x} \tag{40}$$

with Δx being the spatial step size. The right-hand side of equation (38) is solved by a simple Euler step in Δt,

$$T_i^{n+1} = T_i^{n+1,-} + \Delta t \, \frac{\eta_{\text{col}}\eta_{\text{therm}}G}{\rho_i^n c_{v,i} n A} I_i \phi_i^n \,. \tag{41}$$

5 Model for the network of tubes

Equation (38) from the last section describes the flow of a fluid in a single tube. The network of a solar thermal power plant consists of a large number of tubes. To model the whole network, those tubes have to be coupled together. In detail that means specifying how the velocity and the temperature is transported through a junction of tubes. Additionally, the boundary conditions of the network have to be specified. The boundary of the network consists of the pump at the inflow and the heat exchanger at the outflow.

The junctions consist of incoming and outgoing pipes. There are three different types that have to be considered. Outlet-junctions with one outgoing and two incoming pipes (see Figure 4), inlet-junctions with one incoming and two outgoing pipes (see Figure 5) and junctions with one incoming and one outgoing pipe (see Figure 6). The last type exists exactly two times in every solar thermal power plant at the inflow and outflow of the last absorber tube in the network. Every inlet-junction also consists of a valve located at the inflow of the absorber tube adjacent to the junction with an opening factor ξ. All losses inside the junctions and valves will be neglected. Because of this the valve located at the last absorber tube is a special case. The lack of any losses and the fact that no information is transported backwards in the tubes leads to the fact that the opening factor ξ_N of the last valve in the network would have no effect on the flow of the HTF. To solve this problem the position of this valve will be changed. It will be modeled at junction $N-1$. Because of this position the opening factor ξ_N of the last valve has an impact in the flow of the HTF in the network.

5.1 Boundary conditions for the pump and the heat exchanger

An important task when solving a partial differential equation with a finite volume method, is to provide correct boundary conditions. Since the information is only transported in positive x-direction and an upwind-scheme is used, the boundary conditions have to be provided only at the inflow of the network. This means no boundary conditions have to be provided for the heat exchanger. The boundary conditions for the pump will be modeled by setting its volumetric flow q_P and the temperature of the HTF entering the network T_{in}. These are the boundary conditions for the first section of the inflow header-tube. The boundary conditions of every other tube in the network will be provided by the coupling conditions presented in the next section.

5.2 Coupling conditions for the junctions in the network

In Section 4 the behavior of the HTF inside the tube was modeled. In this section equations for the processes inside the junctions connecting the tubes are derived. These are called the coupling conditions. These conditions provide a way of calculating the entry temperature and velocity of the HTF into a tube from a junction dependent on the conditions the HTF entered with. Since an incompressible flow is assumed the velocity in the network depends on the volumetric flow of the pump q_P, the cross

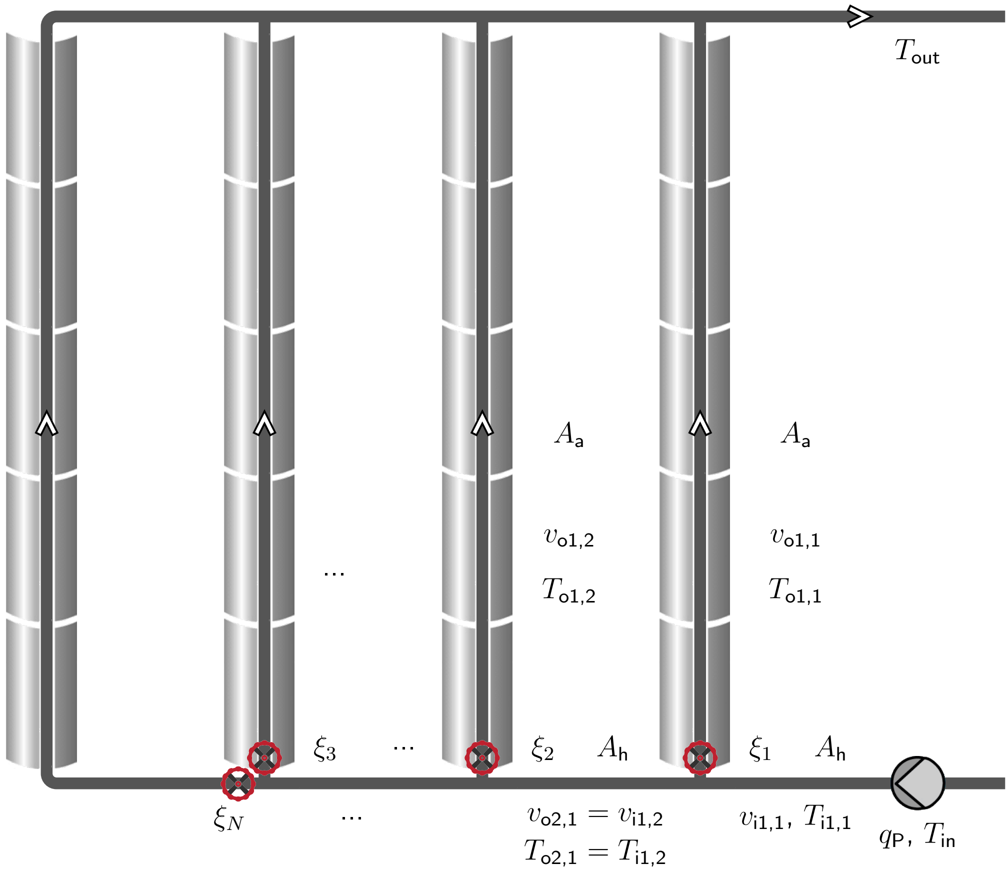

Figure 3: A conceptual drawing of the collector field in a solar thermal power plant with the parameters contained in the network model.

sectional area of the tube A_j and the apertures of the valves in the network ξ_j. It is constant over the length of each tube.
The condition that has to hold at each junction is the conservation of mass [12]

$$\sum A_j \rho_j u_j = 0 \tag{42}$$

with j being the indices for tubes the adjacent to the junction. These indices are $i1$ for the first inflow tube, $i2$ for the second inflow tube, $o1$ for the first outflow tube and $o2$ for the second outflow tube. The unknown parameters are the density ρ_i, temperature T_i and velocity u_i in the outflow tubes $o1$ and $o2$. All other parameters shown in Figure 4, Figure 5 and Figure 6 are known.

5.2.1 Conditions for the velocity in the junctions

As already described we assume the flow of the heat transfer fluid to be incompressible. In this case condition (42) simplifies to

$$\sum A_j u_j = 0\,. \tag{43}$$

To calculate the velocities the three different kinds of junctions have to be considered separately.

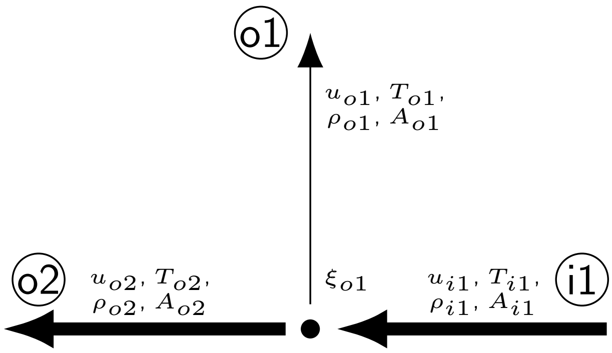

Figure 4: Junction with one incoming and two outgoing pipes. These junctions are always situated at the inflow of the absorber tubes.

Conditions for the velocity in the inlet junctions: In the case of Figure 4 the velocity in pipe o2 u_{o2} and the velocity in the valve of pipe o1 $u_{o1,\xi}$ are identical because all losses were neglected.

$$u_{o1,\xi} = u_{o2} = u_o\,. \tag{44}$$

It can be calculated by condition (43). In order to do that the cross sectional areas of the incoming pipe A_{i1} and the outgoing pipes A_{o1} and A_{o2} have to be specified. The cross sectional areas of pipe i1 and pipe o2 are given by

$$A_{i1} = A_{o2} = A_h\,. \tag{45}$$

The cross sectional area in the valve of pipe o1 is defined by

$$A_{o1} = A_a \cdot \xi_{o1}\,, \tag{46}$$

where A_a is the cross sectional area of the absorber tube and ξ_{o1} is the aperture of the valve located at the inflow of that absorber tube. Altogether this leads to the following expression for the velocity leaving the junction u_o

$$u_o = \frac{A_h u_{i1}}{A_h + A_a \xi_{o1}}\,. \tag{47}$$

The velocity in pipe o1 after the valve can be calculated by

$$u_{o1} = \xi_{o1} u_o \; . \tag{48}$$

As stated before the last inflow valve with two outgoing pipes is a special case. Due to the fact that a valve at the inflow of the very last absorber tube would have no effect on the network, the valve will be modelled at the junction next to the last one. In this case the cross sectional area of pipe o2 becomes

$$A_{o2} = A_a \xi_N \; . \tag{49}$$

The outgoing velocity changes to

$$u_o = \frac{A_h u_{i1}}{A_a(\xi_N + \xi_{o1})} \; , \tag{50}$$

and the velocity in the last section of the header tube is

$$u_{o2} = \frac{u_o \xi_N A_a}{A_h} \; . \tag{51}$$

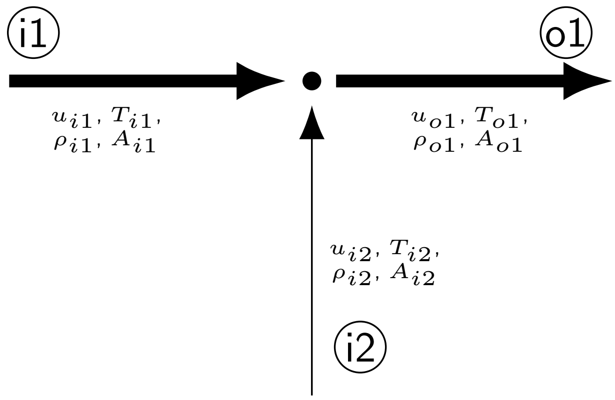

Figure 5: Junction with one outgoing and two incoming pipes. These junctions are always situated at the outflow of the absorber tubes.

Conditions for the velocity in the outlet junctions: In this case the velocities in each pipe are not identical. Velocities u_{i1} and u_{i2} however are known. The cross sectional areas are also given and since there are no valves at the outflow of the absorber tubes they are constant.

$$A_{i1} = A_{o1} = A_h \; , \tag{52}$$

$$A_{i2} = A_a \; . \tag{53}$$

Combined with condition (43) this leads to an expression for u_{o1}

$$u_{o1} = \frac{u_{i1} A_h + u_{i2} A_a}{A_h} \; . \tag{54}$$

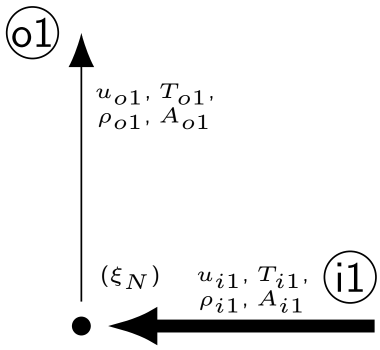

Figure 6: Junction with one incoming and one outgoing pipe. These junctions are situated at the inflow and outflow of the very last absorber tube.

Conditions for the velocity in the last junctions: The last junctions connect the end of the header tubes to the last absorber tube in the network. They exist exactly twice. There is no valve at this type of junction because it was modeled at the junction before this one. With condition (43) the outgoing velocity u_{o1} can be calculated by

$$u_{o1} = \frac{A_{i1} u_{i1}}{A_{o1}} \, . \tag{55}$$

The cross sectional areas A_{i1} and A_{o1} depend on the junction. For the inflow junction they are

$$A_{i1} = A_h \tag{56}$$

and

$$A_{o1} = A_a \, . \tag{57}$$

For the outflow junction they are reversed,

$$A_{i1} = A_a \, , \tag{58}$$

$$A_{o1} = A_h \, . \tag{59}$$

With these conditions the velocities int the network can be calculated by applying them consecutively from the first up until to the last junction of the network, depending on the direction of the flow.

5.2.2 Conditions for the temperature in the junctions

There are two different cases that must be considered when calculating the temperature in the junctions: one incoming pipe and two incoming pipes. The first one means that the temperature of the incoming pipe will be distributed to the outgoing pipes. In the second case two different temperatures are mixed together.

Conditions for one incoming pipe: This case can be applied at all inflow junctions and the last outflow junction, meaning the one connecting the last absorber tube to the outflow header tube. Calculating the temperature for this one is simple. The inflow temperature is equal to the temperatures at the outflows because there is neither energy input nor any losses at the junctions.

$$T_{i1} = T_{o1} = T_{o2} \tag{60}$$

Conditions for two incoming pipes: When there are two different incoming pipes we have to calculate a mixed temperature depending on the temperature of the inflow. This can be done by applying condition (42). The first step is to calculate a mixture density. All incoming densities, velocities and the outgoing velocity are known. Thereby we can derive the following expression for ρ_{o1}.

$$\rho_{o1} = \frac{\rho_{i1} u_{i1} A_h + \rho_{i2} u_{i2} A_a}{u_{o1} A_h} \, . \tag{61}$$

With the mixed density ρ_{o1} we can calculate the mixed temperature T_{o1} by applying the closure equation described in Section 4.2.

6 Mirror control

In this section the state of the art for controlling the temperature in a network of tubes will be presented, which we call the mirror control. The idea behind it is to control the volumetric flow of the pump to keep the outflow temperature for each absorber tube as close as possible to the desired temperature. If that is not possible by controlling the pump alone mirrors will be defocused from the collector field to stop the energy input from the sun. The desired temperature T_{out} is defined by the HTF. A threshold around T_{out} must also be defined. It is needed to make sure the temperature in the absorber-tubes does not cool down too much. Before that the design point of the power plant will be introduced.

6.1 Design point of the power plant

Once a year the network in a solar thermal power plant is set to a specific point, which is called the design point. The valves are being calibrated to an ideal working point so that all the mirrors are being used. For the rest of the year the valves apertures are kept constant even when the weather conditions change.
The design point is calculated at a time when the solar irradiation is constant in all absorber tubes. That means the volumetric flow in each tube has to be equal. This volumetric flow q_{DP} can be calculated. It depends on the length of the absorber tube ℓ_{a}, the solar irradiation at the design point I_{DP}, the inflow temperature T_{in} and the desired temperature T_{out}. Since the design point can be considered as a steady state it follows that $T_t = 0$. Combined with equation (38) this results in

$$uT_x = \frac{\eta_{\text{col}}\eta_{\text{therm}}G}{\rho c_{\text{v}} A_{\text{a}}} I(x) \,. \tag{62}$$

By rearranging and adding $u \cdot A_{\text{a}} = q_{\text{DP}}$ we get

$$q_{\text{DP}}T_x = \frac{\eta_{\text{col}}\eta_{\text{therm}}G}{\rho c_{\text{v}}} I(x) \,. \tag{63}$$

The derivative of the temperature with respect to space can be approximated by a simple central difference between T_{in} and T_{out},

$$T_x = \frac{T_{\text{out}} - T_{\text{in}}}{\ell_{\text{a}}} \,. \tag{64}$$

The solar irradiation $I(x)$ is set to

$$I(x) = I_{DP} \,. \tag{65}$$

The density ρ and specific heat capacity c_{v} are dependent on the temperature and thus change along the length of the absorber tube. Constant values for ρ and c_{v} are assumed,

$$\rho(x) = \rho_{\text{DP}} \,, \tag{66}$$

$$c_{\mathrm{v}}(x) = c_{\mathrm{v,DP}} \; . \tag{67}$$

ρ_{DP} and $c_{\mathrm{v,DP}}$ are calculated iteratively.
Combining equations (63) and (64) and inserting the constant values for the solar irradiation, density and specific heat capacity an expression for the volumetric flow through an absorber tube at the design point is derived,

$$q_{\mathrm{DP}} = \frac{\ell_{\mathrm{a}} I_{\mathrm{DP}} \eta_{\mathrm{col}} \eta_{\mathrm{therm}} G}{\rho_{\mathrm{DP}} c_{\mathrm{v,DP}} (T_{\mathrm{out}} - T_{\mathrm{in}})} \; . \tag{68}$$

The volumetric flow for the pump at the design point $q_{\mathrm{P,DP}}$ can be calculated by multiplying q_{DP} with the number of absorber tubes,

$$q_{\mathrm{P,DP}} = q_{\mathrm{DP}} \cdot N \; . \tag{69}$$

In order to reach q_{DP} in every absorber tube the valves are set to distribute the volumetric flow $q_{\mathrm{P,DP}}$ evenly through all tubes.

6.2 Controlling the pump volumetric flow

The mirror control consists of two parts that are necessary to reach the desired temperature without exceeding it. The control of the pump and the defocussing of mirrors. In this section the strategy for controlling the pump is presented.
The control of the pump verifies that the fluid does not become too cold. Only by decreasing the pump volumetric flow q_{P} can the temperature of the HTF be increased, because it flows more slowly and has a longer time to heat up. Using the controller for the pump without defocussing mirrors from the collector field would result in the HTF in the coolest absorber tube reaching the desired temperature exactly while all other tubes reach the same or a higher temperature.

6.2.1 Designing the controller for the pump

There are a lot of different approaches how to develop a controller for a solar thermal power plant. In this thesis a PID-controller will be used. It is designed with the Ziegler–Nichols tuning method [13]. The goal is to control the pump volumetric flow q_{P} with the temperature deviation ΔT at the end of the absorber tube. The corresponding differential equation for the controller is

$$q_{\mathrm{P}} = K_p \cdot \left(\Delta T + \frac{1}{T_i} \int \Delta T dt + T_d \frac{\partial(\Delta T)}{\partial t} \right) \; . \tag{70}$$

The parameters K_p, T_i and T_d are chosen by Table 4. To use the method the integral and derivative gains must be set to zero. The proportional gain K_p is then set to zero and slowly increased until the output of the control loop shows stable and consistent oscillations. K_u is set to the obtained proportional gain and T_u to the oscillation period of the output.

K_p	T_i	T_d
$0.6K_u$	$T_u/2$	$T_u/8$

Table 4: Ziegler-Nichols method

6.2.2 Distribution of the volumetric flow through the network of tubes

The controller was designed to regulate the temperature in a single absorber tube by changing the volumetric flow through that absorber tube. When a plant consists of more than one absorber tube the question remains how the volumetric flow of the pump must be set to realize the needed volumetric flow in the absorber tubes. Because the model (38) neglects all losses, changes to the volumetric flow of the pump are distributed evenly among all absorber tubes. To achieve the needed volumetric flow in the i-th absorber tube the difference between the old and new volumetric flow in that tube has to be added to the pump volumetric flow multiplied by the numbers of absorber tubes in the plant,

$$q_{\mathrm{P,new}} = q_{\mathrm{P}} + (q_{\mathrm{i,new}} - q_i) \cdot N \,, \tag{71}$$

with N being the number of absorber tubes in the plant.

6.3 Defocussing mirrors from the collector field

In the last subsection a control scheme was introduced that assures the HTF does not get too cold in the absorber tubes. In order to never exceed the desired temperature T_{out} mirrors are being defocused from the collector field.
The increase in temperature over the length of one mirror in an absorber tube $\Delta T_{\mathrm{mirror}}$ is approximated by a simulation. This value is used to calculate the number of mirrors that need to be defocused from the collector row to keep the temperature in the absorber tubes below the desired temperature without defocussing too many mirrors. To achieve this, the difference between the temperature and the desired temperature ΔT_{out} is measured. The number of mirrors that have to be defocused N_{defocus} is calculated by

$$N_{\mathrm{defocus}} = \left\lceil \frac{\Delta T_{\mathrm{out}}}{\Delta T_{\mathrm{mirror}}} \right\rceil \tag{72}$$

The algorithm for defocussing mirrors is shown in Figure 7.

for i=1; i <= N; i++ **do**
  if $T_i < T_{out}$ **then**
    decrease q_P according to equation (71)
  end if
end for
for i=1; i <= N; i++ **do**
  if $T_i > T_{out}$ **then**
    calculate $N_{defocus}$ according to equation (72)
    defocus mirrors
  end if
end for

Figure 7: The algorithm used for defocussing mirrors in the collector field. First the volumetric flow is decreased in a way that the HTF in the tube which is overshadowed the most reaches the desired temperature. For all tubes that exceed the desired temperature at that point the number of mirrors that need to be defocused is calculated and defocused.

7 Valve control

In Section 6 a way of controlling the temperature in the absorber tubes of a solar thermal power plant is introduced. It depends on defocussing mirrors from the collector field to ensure that the HTF does not overheat. The defocussing of mirrors however does have a drawback. Every defocused mirror means a certain loss of energy to the system. To increase the efficiency of the plant it should be the goal to minimize the defocus time of mirrors in the collector field.

In this section another way of controlling the temperature in a solar thermal power plant is introduced, the valve control. It includes using the valves dynamically in the control process. It attempts to decrease the defocus time to zero without allowing the HTF to exceed or fall below the desired interval of the temperature. In order to accomplish this, the system of tubes is decoupled. Decoupling means finding a way of changing the volumetric flow in a single absorber tube of the network without changing the flow in the other absorber tubes by setting the aperture of the valves.

7.1 Decoupling the influence of the pump and the valves on the volumetric flow of each pipe

When regulating a solar thermal power plant an important task is to decouple the pipes. Decoupling means we want to be able to regulate one single pipe without affecting the others. Since the pump volumetric flow and the valves apertures influence all the pipes in the network, we have to derive a scheme for decoupling the pipes.

In order to derive the wanted scheme we first look at the volume flow through the pipes. The volume flow through the first pipe is

$$q_1 = q_\mathrm{P} \frac{A_\mathrm{a}\xi_1}{A_\mathrm{h} + A_\mathrm{a}\xi_1} \tag{73}$$

with q_1 and q_P being the volumetric flow through pipe one and the pump respectively. The volume flows through the second and third pipe are

$$q_2 = A_\mathrm{a} q_\mathrm{P} \frac{A_\mathrm{a}\xi_2}{(A_\mathrm{h} + A_\mathrm{a}\xi_1)(A_\mathrm{h} + A_\mathrm{a}\xi_2)} \tag{74}$$

and

$$q_3 = A_\mathrm{a}^2 q_\mathrm{P} \frac{A_\mathrm{a}\xi_3}{(A_\mathrm{h} + A_\mathrm{a}\xi_1)(A_\mathrm{h} + A_\mathrm{a}\xi_2)(A_\mathrm{h} + A_\mathrm{a}\xi_3)} \,. \tag{75}$$

From these equations a generalized form of the volumetric flow through pipe n is derived,

$$q_n = A_\mathrm{h}^{n-1} q_\mathrm{P} \frac{A_\mathrm{a}\xi_n}{\prod_{i=1}^{n}(A_\mathrm{h} + A_\mathrm{a}\xi_i)} \quad \forall \quad n \in \{1, ..., N-2\} \,. \tag{76}$$

Solving this equation for ξ_n provides an equation for the valves aperture in pipe n dependent on the previous valves apertures, the volumetric flow in pipe n and the pump volumetric flow,

$$\xi_n = q_n A_\mathrm{h} \frac{\prod_{i=1}^{n-1}(A_\mathrm{h} + A_\mathrm{a}\xi_i)}{A_\mathrm{h}^{n-1} A_\mathrm{a} q_\mathrm{P} - A_\mathrm{a} q_n \prod_{i=1}^{n-1}(A_\mathrm{h} + A_\mathrm{a}\xi_i)} \quad \forall \quad n \in \{1, ..., N-2\} \,. \tag{77}$$

The last two valves and absorber tubes are a special case. The apertures of these valves influence only the flow in their respective absorber tubes. The volumetric flows through these tubes can only be derived dependent on one another,

$$q_k = q_\mathrm{in} \cdot \left(1 - \frac{\xi_j}{A_\mathrm{a}(\xi_k + \xi_j)}\right) \quad \forall \quad k, j \in \{N-1, N\} \quad k \neq j \,. \tag{78}$$

q_in is the volumetric flow into the junction where the last two valves are located. It is given by

$$q_\mathrm{in} = q_\mathrm{P} - \sum_{i=1}^{n} q_n \quad \forall \quad n \in \{1, ..., N-2\} \,. \tag{79}$$

Equation (78) solved for ξ_k results in

$$\xi_k = \xi_j \cdot \left(\frac{q_\mathrm{in}}{q_\mathrm{in} - q_k} - 1\right) \quad \forall \quad k, j \in \{N-1, N-2\} \quad k \neq j \,. \tag{80}$$

With equations (77) and (80) it is possible to calculate the aperture of the valve in a specific absorber tube dependent on the desired volumetric flow through that tube.

$q_{diff} = q_n - q_{old,n}$;
$q_P = q_P + q_{diff}$;
for i=1; i<N; i++ **do**
  if $i < N - 2$ **then**
    update ξ_i by equation (77);
  else
    update ξ_i by equation (80)
  end if
end for

Figure 8: The figure shows the algorithm used to achieve the valve control. After the controller calculated the new volumetric flow for absorber tube n the difference between the old and new volumetric flow in this tube is calculated. The pump volumetric flow is updated only by that amount. After the pump is updated the new setting for the valves is calculated by the equations for the decoupled network and applied.

7.2 Applying the decoupling of the valves to control the volumetric flow in the absorber tubes

Because the network can easily be decoupled the outflow-temperature in every single absorber tube can be controlled independently. Some constraints have to be introduced in order to keep the results reasonable. Equation (38) is only valid with a velocity greater than zero. Therefore it is not allowed to close the valves completely. A minimum aperture for the valves has to be defined,

$$\xi > \xi_{\min} \,. \tag{81}$$

The volumetric flow through the pump must also be constrained. A pump in a solar thermal power plant has a specific capacity and can not exceed that. The volumetric flow must also be greater than zero so that the velocity is kept positive.

$$0 < q_{\mathrm{P}} < q_{\mathrm{P,max}} \,. \tag{82}$$

The goal when regulating a network of tubes is essentially to regulate each tube independently of the others. With equations (77) and (80) it is possible to calculate the valves apertures for each tube dependent on the volumetric flow of each tube. That means we can change the volumetric flow in one or more tubes and calculate the valves apertures in a way that the volumetric flow in all the other tubes does not change. This can be achieved by the algorithm shown in Figure 8.

q_n is the new volumetric flow in pipe n which is calculated by the controller. $q_{old,n}$ is the old volumetric flow in pipe n. q_P is the volumetric flow provided by the pump. The concept of this algorithm is to calculate the additionally needed or withdrawn volumetric flow in the tube that requires a change and then adding or withdrawing it from the volumetric flow of the pump. The second step is to adjust the valves in the network in a way, that the added or withdrawn volumetric flow is only transported into the modified absorber tube.

8 Numerical results

In this section numerical simulation test cases are introduced and executed. To validate the results of the model we will simulate a network with a single absorber tube. To show the superiority of the valve control we will simulate a plant with four absorber tubes. We were able to obtain real measurements from the power plant La Africana [14]. From these the test cases are constructed.

8.1 La Africana

La Africana is a concentrating solar thermal power plant in Posadas, Spain [14]. The plant can be seen in Figure 9. The technological properties are given in Table 5 and Table 6. We were able to get real measurements from the operating company of this plant. The data consists of the direct normal irradiation (DNI) for two days, the inflow temperature of a single absorber tube for two days, the outflow temperature of a single absorber tube for two days and the volumetric flow through a single absorber tube for two days. The two days are the 30th and 31st August 2017. The data can be seen in Figure 11, Figure 12 and Figure 13. The DNI on the first day fluctuates heavily, because of clouds overshadowing the plant. It has a more smooth course on the second day. The implemented control schemes are static so a time point has to be chosen. We choose 2:00 PM on the 31st August because it shows a very smooth course. Because of that we can assume that the values are close to a steady state. The values at this time can be seen in Table 7. We choose this as the design point of the solar thermal power plant. The global optical and thermodynamic efficiency must also be set. In [15] typical values for η_{col} and η_{therm} are given (see Table 8). Additionally to the test case with real measurement data we also simulate the plant with four collector rows. We assume the same data as for the test case with a single collector row. Only the volumetric flow will be increased due to the increased number of absorber tubes. Both networks will be simulated with and without partial overshadowing.

Background	
Technology	Parabolic trough
Country	Spain
City	Posadas
Region	Córdoba
Land Area	252 hectares
Solar Resource	1950 MW h per year
Electricity Generation	170 000 MW h per year (estimated)
Start of Production	November 21, 2012

Table 5: Background for solar thermal power plant La Africana in Posadas, Spain. `https://www.nrel.gov/csp/solarpaces/project_detail.cfm/projectID=236`

Figure 9: Complete view of the solar thermal power plant in Posadas, Spain. The large number of collector rows is clearly visible as well as the plant that generates electricity. This plant also consists of two indirect tanks to store the thermal energy in the form of heated fluid to be accessed later. `http://en.grupotsk.com/images/uploads/proyectoimage/408/imagen/at10-199.jpg`

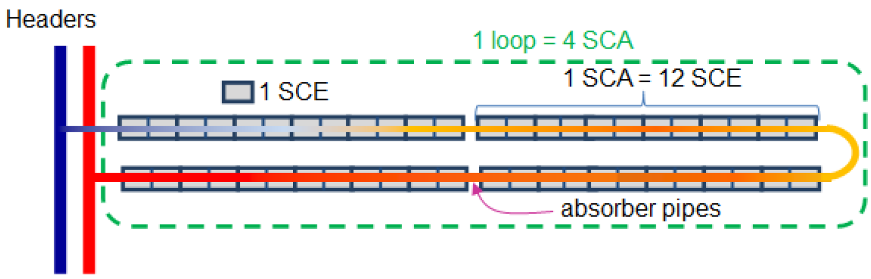

Figure 10: This is a single absorber as they are used in the power plant La Africana. It is called a loop and consists of four solar collector assemblies (SCA). In each SCA there are 12 solar collector elements (SCE). Each SCE is a single mirror. They run in a U-shape to save space and to simplify the routing of the header tubes. `http://www.mdpi.com/1996-1073/8/12/12373/htm`

8.2 Results for the network with one collector row

In this section the test cases and the results for the network with a single collector row are presented. They include the design point of the plant, the mirror control with partial overshadowing and the valve control with partial overshadowing. This test case was constructed to validate the results of the simulation.

Plant configuration	
Solar-Field Aperture Area	550 000 m^2
# of solar collector assemblies (SCAs)	672
# of absorber tubes	168
# of SCAs per absorber tube	4
SCA length	150 m
# of mirrors per SCA	12
Length of the absorber tube ℓ_a	600 m
Aperture of the mirrors G	5,45 m

Table 6: Plant configuration for the solar thermal power plant La Africana in Posadas, Spain. `https://www.nrel.gov/csp/solarpaces/project_detail.cfm/projectID=236`

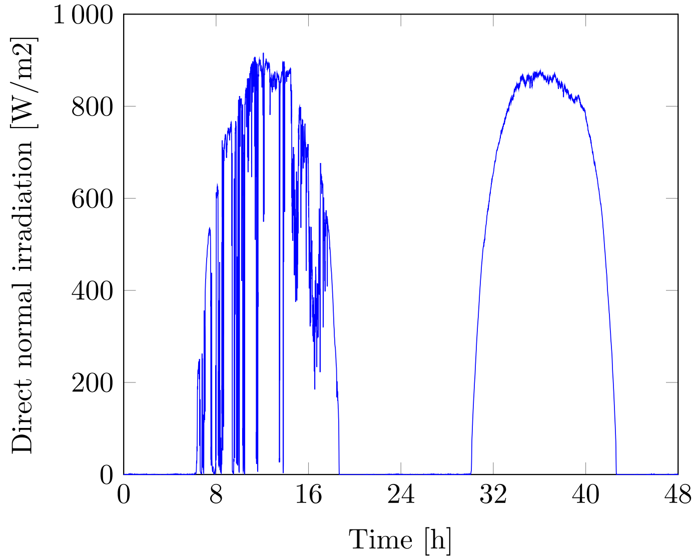

Figure 11: The figure shows the direct normal irradiation over the power plant La Africana over the course of two days. The days chosen were the 30th and 31st August 2017. It is visible that the direct normal irradiation fluctuates heavily on the first day while it has a very smooth course on the second. The fluctuations are due to overshadowing by clouds. The 31st was a day with clear weather.

8.2.1 Design point

The design point is the ideal working point of the solar thermal power plant. In this sense, no shadows are considered when simulating the design point. Since only one absorber tube is simulated in this test case the valve has no impact. To reach the desired temperature the volumetric flow of the pump is set. This setting should lead to a strictly positive increase of the temperature in the absorber tube. The results shown in Figure 14 verify that the simulation code is correct. It can be seen that

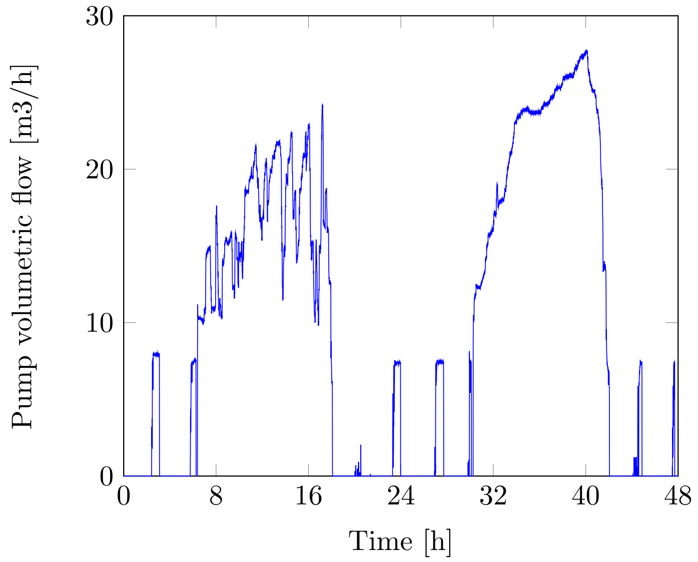

Figure 12: The figure shows the mass flow in the single absorber tube of the power plant La Africana over the course of two days. The days chosen were the 30th and 31st August 2017. The volumetric flow on the 30th fluctuates more which is caused by the fluctuations in the direct normal irradiation. The 31st shows a more even course.

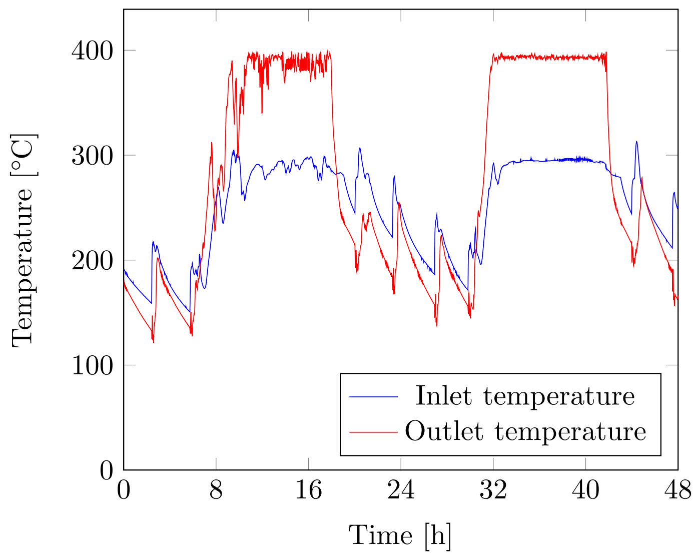

Figure 13: The figure shows the inlet and outlet temperature of the power plant La Africana over the course of two days. The days chosen were the 30th and 31st August 2017. The temperature on the 30th fluctuates heavily around the desired temperature which is due to the changes in the volumetric flow. The temperature on the 31st is very smooth.

Parameter	Value
Direct normal irradiation	843,5 $\mathrm{W\,m^{-2}}$
Inflow Temperature T_{in}	294,42 °C
Outflow Temperature T_{out}	393,21 °C

Table 7: The values of the data shown in Figure 11 and Figure 13 at 2:00PM, 31st August 2017

Efficiency type	Value
Optical η_{col}	0,75
Thermodynamic η_{therm}	0,7

Table 8: The optical efficiency and thermodynamic efficiency for the collector field and HTF.

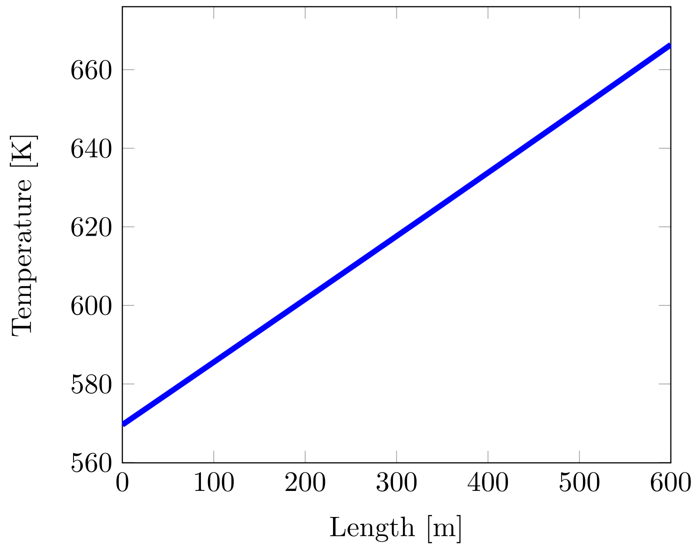

Figure 14: Simulation results for one collector row with no partial overshadowing and no control mechanism. The temperature increases over the length of the tube and reaches exactly the desired temperature. This is the design point.

the temperature increases over the length of the single absorber tube. It reaches the desired temperature exactly at the end of the tube. This state is the constructed design point of the plant with one absorber tube. The volumetric flow through the tube is 28,44 $\mathrm{m^3\,h^{-1}}$. The measured value at this time point is 11% lower at 25,3 $\mathrm{m^3\,h^{-1}}$. This shows that the model definitely tends to the correct value for the volumetric flow. The difference can be explained by the lack of knowledge about the real efficiency factors of the power plant. It is also possible that some of the mirrors in the collector row of the real power plant are defocused which would result in a reduced volumetric flow.

For testing the control schemes shadows were simulated over the collector row. The shadow distribution is shown in Figure 15. Under the assumption that no energy is

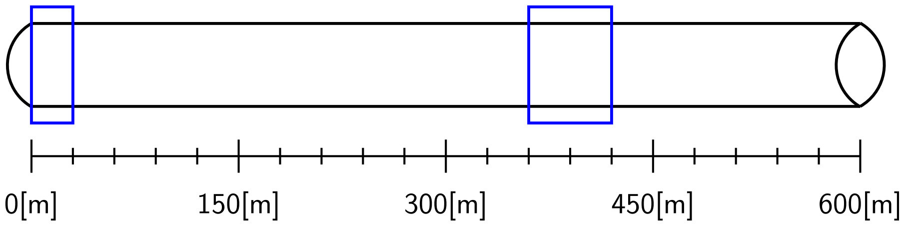

Figure 15: A conceptual drawing of a partially overshadowed tube. The blue rectangles represent the shadows. This is the shadow setting for the test case.

transported into the HTF if the mirror is overshadowed, the solar irradiation was set to zero in these parts. The solar irradiation stays constant in the not overshadowed parts of the collector row with the value used to calculate the design point.

8.2.2 Mirror control

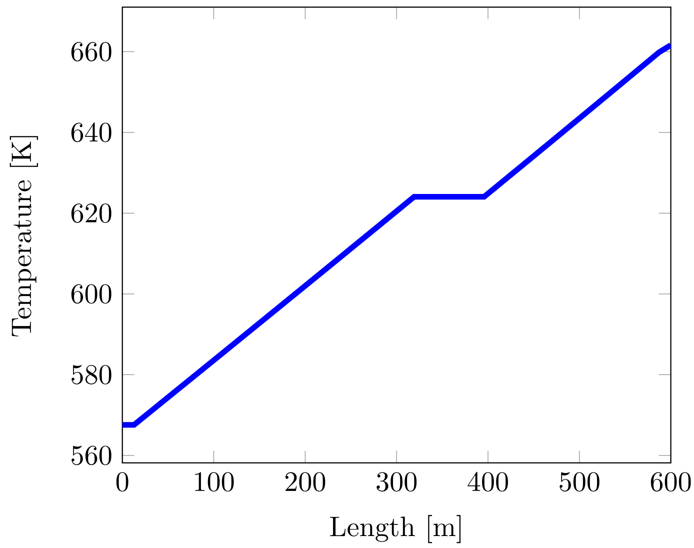

Figure 16: Simulation results for one collector row with partial overshadowing and the mirror control mechanism. In the overshadowed parts the temperature does not increase because the solar irradiation was set to zero. The pump volumetric flow was decreased to reach the desired temperature.

To test the mirror control a single partially overshadowed absorber tube was simulated. Other than the presence of shadows and the use of a control scheme the setting is the same as in Section 8.2.1. In the overshadowed parts of the tube the temperature should not increase due to the fact that the solar irradiation was set to zero. The not overshadowed parts should have a slightly steeper increase in temperature to still be able to reach the desired temperature. Since this network consists of only one tube no mirror should be defocused. The controller of the pump should be sufficient for the

HTF to reach the desired temperature.
The results of the mirror control are shown in Figure 16. In the overshadowed parts of the tube, the temperature is constant. In comparison to the design point the volumetric flow of the pump q_P was decreased to $24{,}56\,\mathrm{m^3\,h^{-1}}$ to slow the flow of the HTF. This is expected because the energy input to the system is decreased due to shadows over the collector field. The outlet temperature is 388,47 °C. It is about 5 °C lower than the desired temperature shown in Table 7. This is due to the fact that the mirror control was designed to keep the outlet temperature in a certain interval under the desired temperature.

8.2.3 Valve Control

To be able to compare the results of the valve control and mirror control the valve control uses the same setting as the mirror control. The expectations in the results are also the same. The valve in the network has no impact so the pump is the only controllable part of the plant. The results shown in Figure 17 correspond with the

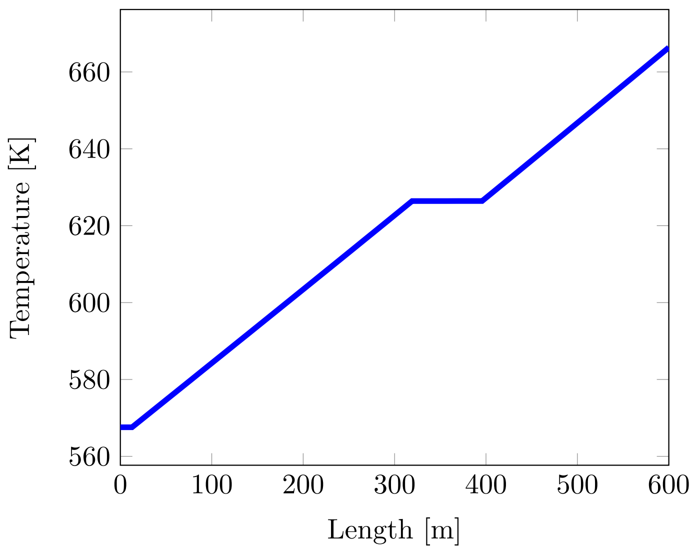

Figure 17: Simulation results for one collector row with partial overshadowing and the valve control mechanism. In the overshadowed parts the temperature does not increase because the solar irradiation was set to zero. The pump volumetric flow was decreased so that the temperature at the end of the tube is exactly the wanted temperature.

valve control. The overshadowed parts of the tube show a horizontal temperature course. The volumetric flow is $23{,}56\,\mathrm{m^3\,h^{-1}}$. The outlet temperature is 393,21 °C. The volumetric flow is 4% lower than the volumetric flow achieved with the mirror control. This difference comes from the fact that the valve control is able to reach the desired temperature exactly but in order to do that the volumetric flow has to be decreased.

This is a desirable effect since it is always the goal of solar thermal power plants to maximize the temperature of the HTF.

8.3 Results for the network with four collector rows

In this section the test cases and results for the network with four absorber tubes are presented. They include the design point, the mirror control with partial overshadowing and the valve control with partial overshadowing. These test cases are constructed to show the improvement the valve control brings in comparison to the mirror control.

8.3.1 Design point

When simulating the design point for a network of tubes with more than one absorber tube the valves have to be set as well as the volumetric flow of the pump. The goal is to set the volumetric flow through each absorber tube to the same value. This should lead to a setting where the increase in temperature is the same in every tube.

Figure 18 shows the design point for a solar thermal power plant with four collector

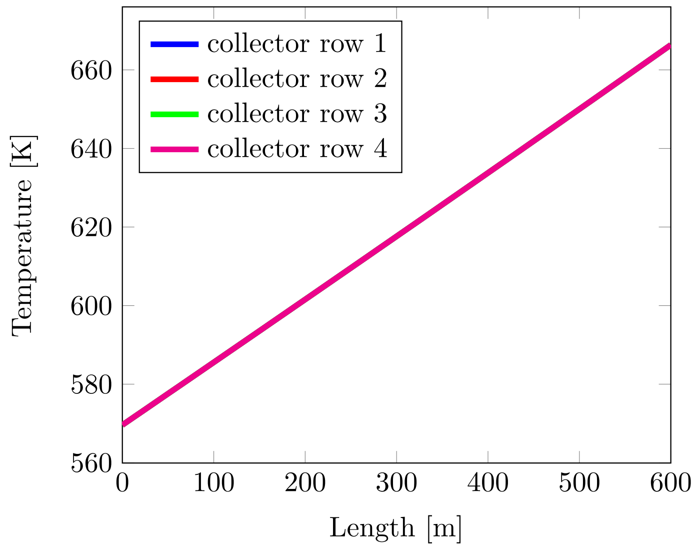

Figure 18: Simulation results for four collector rows with no partial overshadowing and no control mechanism. The temperature distributions in all four tubes are the same. The valves and pump volumetric flow were set to achieve exactly that. This is the design point.

rows. There is no partial overshadowing and the plant is set to a point where all absorber tubes reach the desired temperature. This leads to the expected temperature distribution. The volumetric flow of 113,08 $\mathrm{m^3\,h^{-1}}$ is the maximum flow the plant can reach with the solar irradiation shown in Table 7.

Figure 19 shows the chosen distribution of shadows over the four collector rows of the collector field for the following test cases. The first absorber tube is the one located

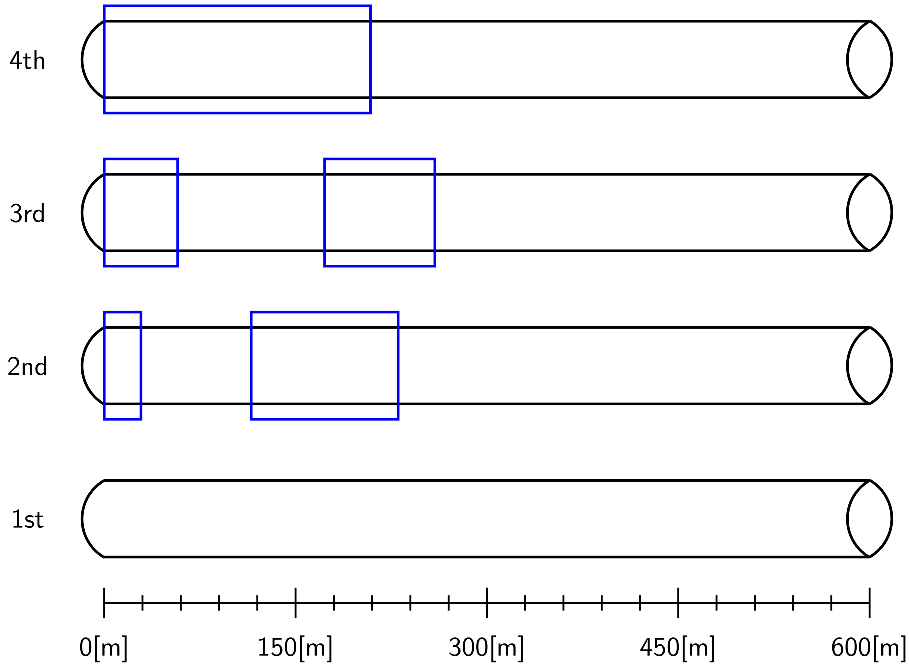

Figure 19: A conceptual drawing of four partially overshadowed absorber tubes. The blue rectangles represent the shadows. This is the shadow setting for the test case with four absorber tubes.

closest to the pump while the fourth tube is the farthest. The HTF enters the absorber tubes on the left side and leaves them on the right.

8.3.2 Mirror control

In this test case the mirror control is used to control the temperature in the network with four absorber tubes. The overshadowed parts of the network should show no increase in temperature. In addition, the temperature of the HTF should stay constant at the end of the first, second and third absorber tube. It is expected that mirrors will be defocused at the end of these tubes to keep the temperature in the interval of the desired temperature. In the fourth tube no mirror should be defocused because it is overshadowed the most so the volumetric flow of the pump will be set in a way that the HTF in this tube reaches the desired temperature exactly. As can be seen in Figure 20 the overshadowed parts of the collector field show a horizontal course of the temperature. At the end of the first until the third absorber tube the temperature does also not increase. In these parts of the collector field the mirrors were defocused so that there is no energy input to the tubes. For the fourth tube no mirror was defocused because it is the coldest tube. The fewer a single tube is overshadowed the more mirrors must be defocused to assure the temperature stays in the desired interval. The volumetric flow of $77{,}96\,\mathrm{m^3\,h^{-1}}$ is significantly lower than for the design point. This is due to the energy loss of the overshadowed parts of the collector field

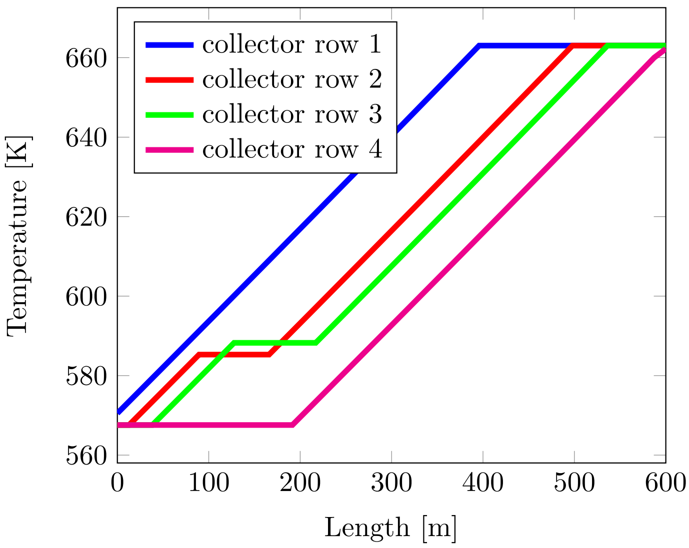

Figure 20: Simulation results for four collector rows with partial overshadowing and the mirror control mechanism. All four tubes reach almost the correct temperature. Due to the implementation of this control scheme there are some slight variations. The pump volumetric flow is decreased until the coldest tube reaches the correct temperature. In every other tube enough mirrors are defocused so that they do not exceed the maximum temperature.

and the defocused mirrors. A total of 29 mirrors have been defocused. The outlet temperature of the network into the heat exchanger is 389,65 °C. It is slightly lower than the desired temperature because of the fact that the temperature is kept in a certain interval under the desired temperature.

8.3.3 Valve control

This test case utilizes the advancement that is the valve control. Every tube is overshadowed in a different way and a different length. As was shown in the previous section this leads to each tube reaching a different temperature if no mirror is defocused. When using the valve control the temperature distribution is expected to be different. Since the volumetric flow through each absorber tube is not equal anymore the course of the temperatures in the absorber tubes should not be parallel. The overshadowed parts of the tubes should still show a horizontal course. Other than that, the temperature of the HTF should reach the desired value in each tube with a different gradient. Figure 21 shows the results of the valve control for this test case. Only the overshadowed parts of the tubes display a horizontal course due to the lack of energy input. Since no mirrors were defocused and the volumetric flow through each tube was set independently the desired temperature is reached in all tubes. The different volumetric flows through the tubes are visible by the different gradients of the temperature distributions. The overall volumetric flow of 92,46 $\mathrm{m^3\,h^{-1}}$ is 18.6% higher than with the mirror control. The outlet temperature of the network is 393,21 °C. This is exactly

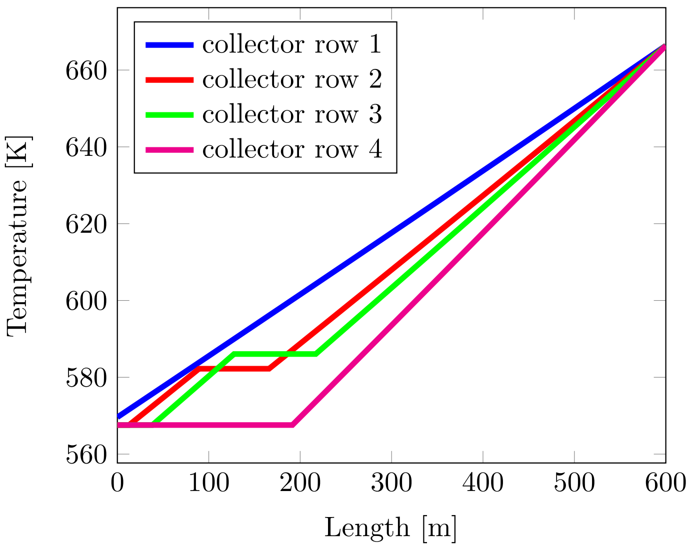

Figure 21: Simulation results for four collector rows with partial overshadowing and the valve control mechanism. Every tube reaches the wanted temperature without any defocused mirrors. The valves are set to this specific point. This yields a higher mass flow at the maximum temperature.

the desired temperature shown in Table 7. The only energy loss to the system comes from the shadows over the collector field. The increase in temperature and volumetric flow by using the valve control in comparison to the mirror control is a significant improvement to the efficiency of the solar thermal power plant.

9 Conclusion

The task of this thesis was to develop and to improve the state-of-the-art control of the temperature in a network of tubes of a solar thermal power plant with parabolic trough technology. To achieve this, the energy input from the sun, the flow of the HTF and the network of tubes were modeled. The obtained equation for the fluid was solved with a finite volume method. A controller for the pump volumetric flow was developed as well as an algorithm for defocussing mirrors from the collector field, called the mirror control. The influence of the pump and the individual valves was decoupled from the system, making possible a way of controlling the temperature in the absorber tubes without defocussing any of the mirrors from the collector rows. This was accomplished by controlling the aperture of the valves at the inflow of each absorber tube individually to change the volumetric flow of a single absorber tube without influencing the other tubes. The new approach was called the valve control. Two test cases were constructed from real measurements to verify the implementation and compare the results.
This comparison revealed that the newly developed valve control yields 18.6% more volumetric flow of heated fluid over the state-of-the-art approach of defocussing mirrors when using a power plant with four absorber tubes. This is a significant increase which shows that the valve control is superior to the mirror control. The goal of increasing the efficiency of solar thermal power plants was met. The improvement is further supported by the fact that the technology to use the new valve control scheme is already available in real solar thermal power plants.

Outlook

Because the developed control mechanism is static the next step should be to implement a dynamic control scheme. This would also have to include a predictive part since the effect of overshadowing clouds on the temperature is much faster than the effect of the valves on the flow of the fluid and thus on the temperature. It is also important to further validate the results with realistic test cases. An immense step would be to implement and test the control scheme in a real solar thermal power plant to be able to obtain real measurements and see if the theoretical improvement is applicable to real solar thermal power plants.

References

[1] Kenneth Karlsson, Stefan Petrovic, and Diana Abad Hernando. Global outlook on energy technology development. *DTU International Energy Report 2018*, page 21, 2018.

[2] J Sawin et al. Renewable energy policy network for the 21st century renewables 2017 global status report. *REN21 Secretariat: Paris, France*, pages 1–302, 2017.

[3] Eduardo F. Camacho, Manuel Berenguel, Francisco R. Rubio, and Diego Martínez. *Control of Solar Energy Systems*. Advances in Industrial Control. Springer-Verlag London, 1 edition, 2012.

[4] Julio Elias Normey-Rico and Eduardo Fernandez Camacho. Control of dead-time processes. *Time (minutes) Time (minutes)*, 2007.

[5] Sarah Mechhoud and Taous-Meriem Laleg-Kirati. Source term boundary adaptive estimation in a first-order 1d hyperbolic pde: Application to a one loop solar collector through. In *American Control Conference (ACC), 2016*, pages 5219–5224. IEEE, 2016.

[6] Parfenov Evgeny. *Zur Modellierung und Simulation eines Parabolrinnenkraftwerkes*. PhD thesis, University Hamburg, 2011.

[7] Manohar S Sohal, Matthias A Ebner, Piyush Sabharwall, and Phil Sharpe. Engineering database of liquid salt thermophysical and thermochemical properties. Technical report, Idaho National Laboratory (INL), 2010.

[8] Therminol Heat Transfer Fluids by Solutia. Inc. therminol vp 1, 2012.

[9] Belgium IFAC Symposium. *Power Systems: Modelling and Control Applications. Selected Papers from the IFAC Symposium Brussels Belgium, 5–8 September 1988*. I F a C Symposia Series. Elsevier Ltd, Pergamon Press, 1 edition, 1989.

[10] Tor A Johansen and Camilla Storaa. Energy-based control of a distributed solar collector field. *Automatica*, 38(7):1191–1199, 2002.

[11] István Farkas and István Vajk. Internal model-based controller for a solar plant. *IFAC Proceedings Volumes*, 35(1):49–54, 2002.

[12] Jens Brouwer, Ingenuin Gasser, and Michael Herty. Gas pipeline models revisited: model hierarchies, nonisothermal models, and simulations of networks. *Multiscale Modeling & Simulation*, 9(2):601–623, 2011.

[13] Anthony S McCormack and Keith R Godfrey. Rule-based autotuning based on frequency domain identification. *IEEE transactions on control systems technology*, 6(1):43–61, 1998.

[14] NREL. La africana solar thermal plant: parabolic trough technology. `https://www.nrel.gov/csp/solarpaces/project_detail.cfm/projectID=236`, 2012. Accessed: 2018-07-25.

[15] MJ Montes, A Abánades, JM Martínez-Val, and M Valdés. Solar multiple optimization for a solar-only thermal power plant, using oil as heat transfer fluid in the parabolic trough collectors. *Solar Energy*, 83(12):2165–2176, 2009.